JOURNAL OF MATERIALS SCIENCE 37 (2002) 4285–4298

Unalloyed copper inclusions in ancient bronze artefacts

C. BOSI, G. L.GARAGNANI
Department of Engineering, University of Ferrara via Saragat, 1-44100 Ferrara, Italy
V. IMBENI, C. MARTINI*
Institute of Metallurgy, University of Bologna, via Risorgimento, 4-40136 Bologna, Italy
E-mail: mart@bomet.fci.unibo.it
R. MAZZEO
ICCROM (International Centre for the Study of the Preservation and Restoration of Cultural Property), via di San Michele, 13-00153 Roma, Italy
G. POLI
Institute of Metallurgy, University of Bologna, via Risorgimento, 4-40136 Bologna, Italy

Ancient bronze artifacts, that represent a considerable part of the archeological finds, have been largely studied because of their complex degradation phenomena taking place in the long time span that have not been fully understood. One of the peculiar features of ancient bronzes is the presence of inclusions of copper unalloyed with tin. Unalloyed Copper Inclusions (UCI) have been observed in buried archaeological bronze artefacts by several authors, but each paper reports only on a limited number of cases. In our extensive studies on bronze artefacts, UCI have been observed in many bronze artefacts with very different features and purposes. Both as-cast and wrought artefacts were studied, so that the influence of the manufacturing process and the composition of the artefacts on the formation of UCI might be evaluated. The microstructure and composition of these artefacts were studied and the features of UCI have been related with those of the surrounding phases. The results have been discussed and compared with those obtained by other authors. The presence of UCI in buried archaeological bronze artefacts could indicate some unusual corrosion processes that might need to be accounted for when designing conservation treatments.

1. Introduction

The study and comprehension of corrosion phenomena in archaeological and ancient metal artefacts is of great importance for both the archaeologist ('past perspective') and the conservation scientist ('present-future perspective'): the former can achieve a better understanding of the level of civilisation and technology in a given time and place, the latter will be able to define appropriate methodologies for protection and solutions to avoid, prevent, and reduce deterioration processes. Also, 'naturally' corroded samples coming from a burial environment where they have been for centuries are of great interest for long-term corrosion studies as most laboratory experiments only last for months and long-term data are otherwise obtained by simulation or extrapolation. One of the peculiar features of ancient bronzes is the presence of inclusions of copper unalloyed with tin (Unalloyed Copper Inclusions, henceforward UCI) that have been observed by several authors in buried archaeological bronze artefacts [1–11]: a list of cases is summarised in Table I.

Most authors explain the formation of copper inclusions in bronze objects by a corrosion-redeposition mechanism, somewhat akin to the process of dezincification in α/β brasses. Dezincification leads to the formation of the so-called "redeposited copper" inclusions: copper precipitates as a result of the selective corrosion of the β phase [12]. Redeposition of copper also occurs in aluminium bronzes when exposed to seawater or fresh water ("dealuminification"), but this phenomenon has never been observed in modern tin bronzes [5]. This suggests that the redeposition of copper is (i) kinetically slow and/or (ii) takes place only in specific environmental conditions. The term "destannification" has been proposed for the formation of unalloyed copper because of the analogy with dezincification [5].

The earlier explanations [2] claim that unalloyed copper inclusions are the result of "localised electrolytic

*Author to whom all correspondence should be addressed.

TABLE I Unalloyed copper inclusions (UCI) described in the literature

Artefact	Sn (wt%)	Pb (wt%)	Unalloyed copper	Ref.
Bronze helmet found in the sea near Corfu	–	–	Crystals of metallic copper in the corrosion patina	[1]
Chinese bronze *Hu* ceremonial vessel (Chou dinasty)	21.8	4.1	Irregular islands that replace Pb droplets in the corroded $\alpha + \delta$ eutectoid	[2]
Solder lump on the handle of Chinese bronze *Kuei* ceremonial vessel	21	9	Globules that replace Pb droplets in the corroded $\alpha + \delta$ eutectoid	[2]
Anglo-saxon square-headed brooch; gilded bronze (from the cemetery at Lechlade Butlers Field, Gloucestershire)	n.d.	n.d.	Redeposited copper patch ("brown stain") over the gilding	[3]
Thai circular bronze bracelet (Ban Chiang, 500 B.C.)	5.4	–	Small scattered blobs in the eutectoid regions, surrounded by Cu sulphides	[4]
Luristan bronze dagger (Iran)	20	–	Irregular patches in the interdendritic spaces	[4]
Ecuadorian gilded copper ceremonial axe (Pindilig)	–	–	Grains in the corroded area under the gold coating	[4]
Borchia of Quinto Fiorentino (Italy, 800 B.C.)	8.20	1.26	n.d	[5]
Statue of the Efebo of Selinunte (Italy, 600 B.C.)	8.99	0.70	Twinned grains	[5]
Roman statue of the Emperor Julius Claudius Germanicus (I century A.C.)	11.09	0.82	Irregular patches in the interdendritic spaces	[5]
Mediaeval bell	24.92	0.84	n.d.	[5]
Mesopotamian bronze shaft-hole axe (Hasanlu, 3rd millennium B.C.)	10	n.d.	Metallic Cu in the outer layers of corrosion products	[6]
Chinese general black mirror	n.d.	n.d.	Pure copper grains in the surface layers	[7]
Chinese bronze mirror with zodiacal animals (Sui dinasty, 600 B.C.)	24	Some Pb	Round structures where redeposited Cu is replacing cuprite formed in place of Pb globules; linear areas where redeposited Cu is replacing cuprite in the outer layers of corrosion	[8]
Chinese bronze bell (tomb of the Marquis of Cai, Shou Xian, 450 B.C.)	Moderately high tin	Some Pb	Round structures where redeposited Cu replaces cuprite formed in place of Pb globules; linear areas where redeposited Cu replaces cuprite in the outer layers of corrosion	[8]
Chinese *Wu* State weapons (late Western *Zhou*, Spring and Autumn and Warring States period)	15.3	4.3	Globular particles in Pb particles; filaments in cracks or under corrosion products or at grain boundaries; twinned grains	[9]
Chinese money tree (*yaoquianshu*) from the Eastern *Han* dinasty (AD 25–220)	17	8	Cuprite globules (corroded redeposited copper) that replace Pb globules	[10]
Chinese *Jin* bronzes (vessels and horse fittings), *Zhou* dinasty	–	–	Interdendritic particles replacing eutectoid, globular particles that took over Pb particles; copper filled cracks; surface layers (objects exposed to alkaline soil).	[11]

n.d. = not described

process." According to [4], preferential corrosion of the tin-rich phase of the $\alpha + \delta$ eutectoid leads to the reduction of copper. Specifically, the corrosion-redeposition mechanism is favoured (i) by the depletion of oxygen due to the build-up of over-layers of corrosion products and (ii) by the presence of chloride ions in the burial environment [8].

Some authors [5] also suggest that the redeposition of copper might also have taken place into the cavities left by shrinkage. According to a different explanation [4], unalloyed copper prills could form during casting because of poor mixing of copper and tin.

Most of the publications on this subject simply describe the morphology of unalloyed copper encountered during the study of few artefacts [1–10]. For this reason, the formation of UCI has usually been ascribed to the phenomena that were observed in the specific case of study (corrosion or poor mixing), without a systematic classification. In our extensive studies on a variety of bronze artefacts, UCI have been observed in objects with very different features and purposes. Both as-cast and wrought bronze artefacts with different microstructures have been studied, and different types of UCI have been identified. UCI have been classified on the basis of

TABLE II Objects from the Italian "Terramare" culture (XVI-XIII century B.C.)

Artefact	Sampling	Sn (wt%)	Pb (wt%)	Fe (wt%)
R1: sword (from Redù)	From the blade	10.7	0.26	0.12
R2: "wheel" brooch (from Redù)	From the wheel	14.4	0.27	0.21
R8: knife (from Redù)	From the blade	12.4	0.20	0.05

Copper to balance.

TABLE III Chinese bronze vessels from the Zhouyuan site, late period of Western Zhou (VI-VII century B.C.). Alloy composition from Ref. [13]

Artefact	Sampling	Sn (wt%)	Pb (wt%)	Fe (wt%)
1A: *Hu* vessel	From the ear ring on one handle	7.0	8.2	0.07
1B: *Zun* vessel	From the mouth edge	13.3	0.15	0.78

Copper to balance.

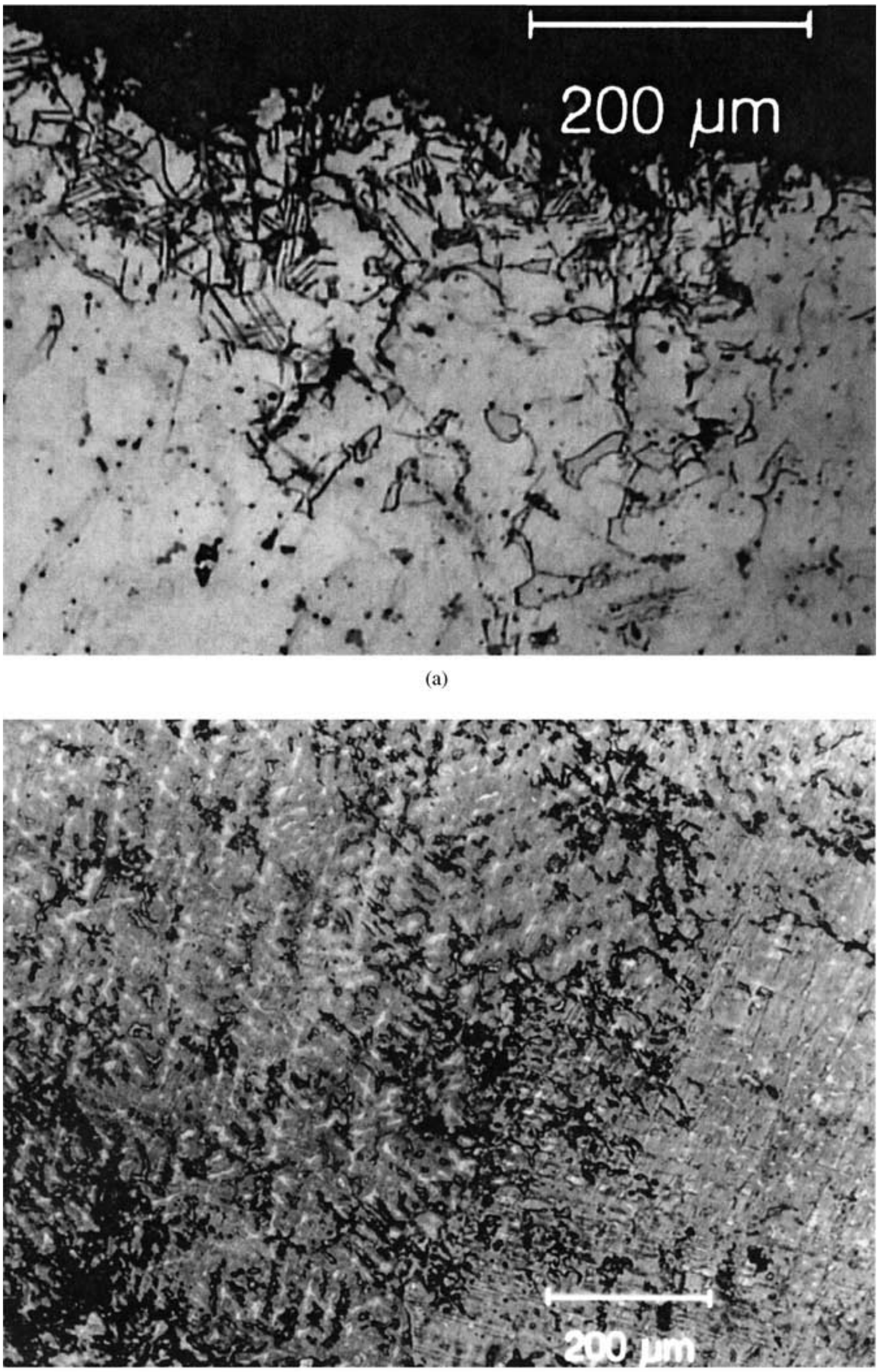

(a)

(b)

Figure 1 Corrosion reveals slip bands in the outer zones of the blade of the knife R8 (a, unetched) but the core region of the weapons has a dendritic structure (sword R1, (b, etched with $FeCl_3$/HCl/ethanol)).

their morphology and a mechanism has been proposed for the formation of each class of UCI.

2. Experimental

Copper inclusions have been observed in brooches and weapons of the Terramare culture (XVI–XIII century B.C.) from Northern Italy as well as in Chinese bronze wine vessels (VI–VII century B.C.). The artefacts are briefly described in Tables II and III respectively. Very small samples (1–3 mm^3) were taken from the artefacts using a fine jeweller's saw. In some cases samples were taken from two or more areas on a single object to check the homogeneity of the microstructure. The samples listed in Tables II and III were mounted and polished for metallographic analysis; samples were observed both before and after etching with $FeCl_3$ (2 g) and HCl (10 mL) in ethanol (about 100 mL).

The microstructure of the samples was studied by optical microscopy (OM), reflected polarised light optical microscopy (RPLMO) and scanning electron microscopy (SEM). Energy Dispersive Spectroscopy (EDS), coupled with SEM, was used for localised compositional microanalyses. Samples for wet chemical quantitative analysis (about 0.01 g) were also taken by drilling into the bronze with small high-speed twist drills (2 mm diameter). Care was taken to get the

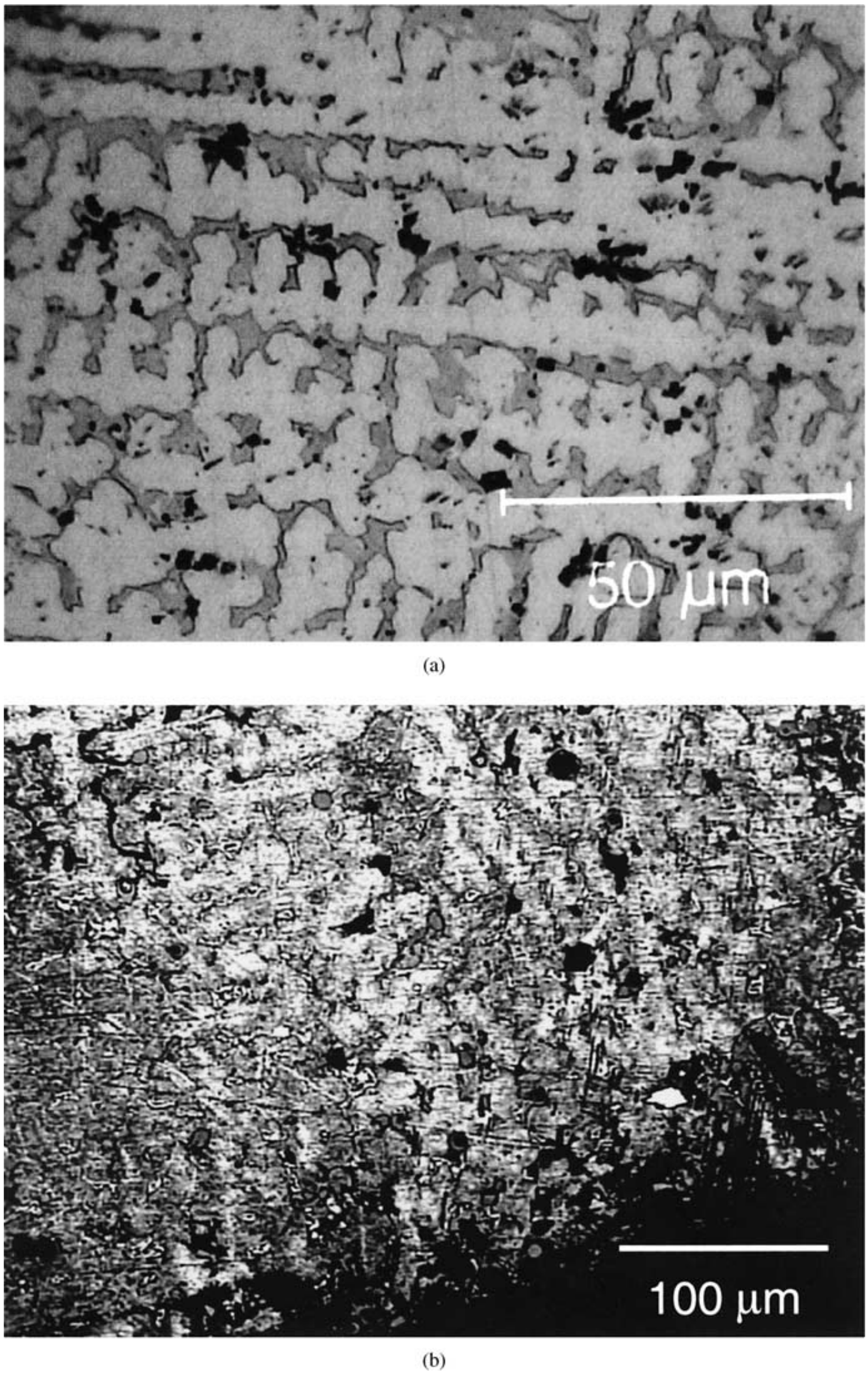

Figure 2 Copper-rich α-phase matrix and $\alpha + \delta$ eutectoid patches in the interdendritic spaces in the brooch R2 (a, unetched) and in the *Zun* vessel 1B (b, etched with $FeCl_3$/HCl/ethanol).

samples from the uncorroded core metal. Flame Atomic Absorption Spectroscopy (FAAS) was used to determine the chemical composition of the samples according to the method described in [14].

3. Results

The sword R1, the brooch R2 and the knife R8 are all tin bronze artefacts (Table II), coming from the same settling, the "Terramara" village of Redù' [13] (Modena, Italy). Other objects from the same site were studied [15], but none of them showed the presence of UCI.

The Chinese *Hu* vessel can be defined as a leaded tin bronze, whereas the *Zun* vessel contains only a small amount of lead (Table III). It is a common knowledge that lead was frequently added to Chinese bronze casting alloys, in order to increase the fluidity of the molten bronze that was poured into ceramic piece-moulds [8].

3.1. Microstructure

The microstructure of Chinese vessels 1A and 1B, and the brooch R2 was completely dendritic. Twinned grains and slip bands were present in the blades of the sword (R1) and the knife (R8), in the regions close to the surface of the object, but the core regions had a dendritic microstructure (Fig. 1). All the bronze artefacts in Tables II and III had a copper-rich α-phase matrix and $\alpha + \delta$ eutectoid patches in the interdendritic spaces (Fig. 2). Segregation of tin in the outer zones

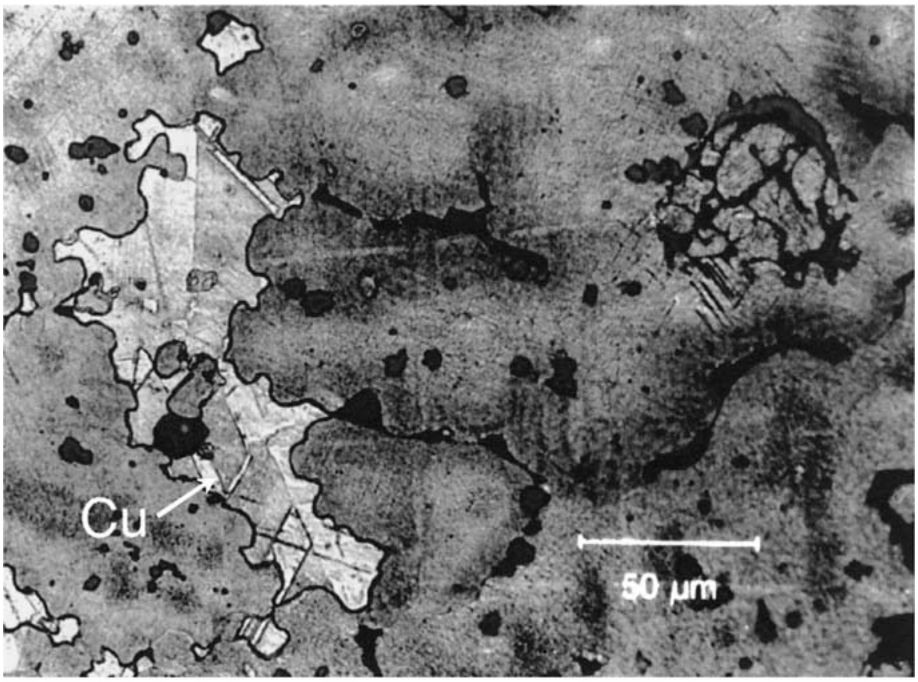

(a)

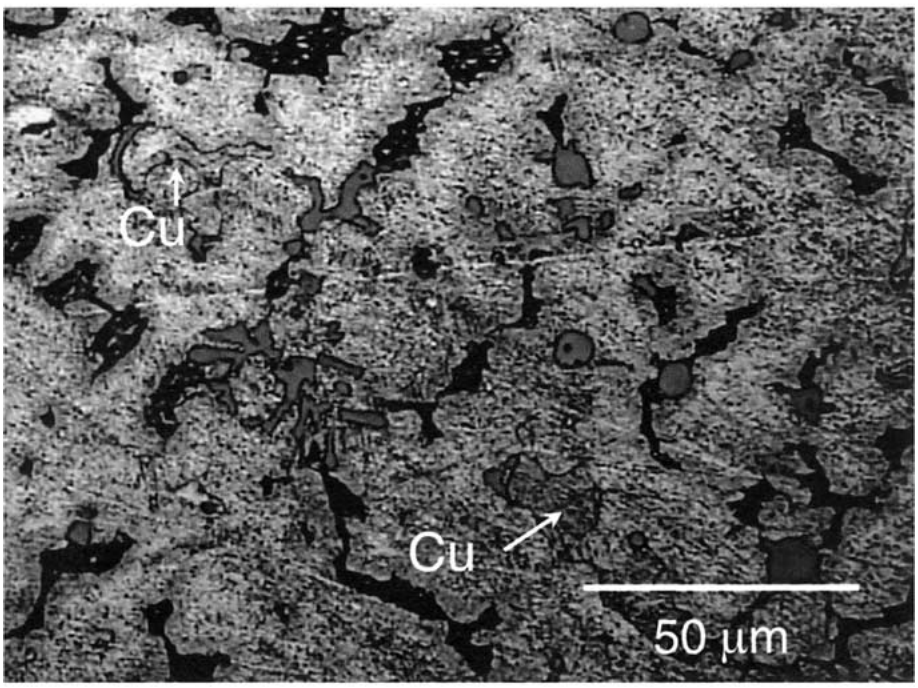

(b)

Figure 3 Coring in the sword R1 (a) and in the *Zun* vessel 1B (b), both etched with $FeCl_3$/HCl/ethanol; unalloyed copper inclusions are labelled "Cu".

Figure 4 Copper sulphide inclusions (dark grey patches) in the *Zun* vessel 1B, etched with $FeCl_3$/HCl/ethanol.

of α-phase dendritic arms also occurred in the Chinese vessels 1A and 1B as well as in the core regions of the Italian weapons R1 and R8 (Fig. 3). The microstructure of the brooch R2, on the other hand, was more homogeneous. As the brooches were probably produced by investment casting and solidified more slowly than the other objects, the cooling process led to the formation of a "close to equilibrium" structure. A large number of non-metallic inclusions were observed in all the examined artefacts (Fig. 4); EDS analyses proved that they were copper sulphides.

Extensive intergranular and interdendritic corrosion was observed on all the artefacts. The blade of the knife R8 also showed some intergranular cracks (Fig. 1a). In the two-phase structures, the tin-rich phase has been preferentially attacked and the α-phase was the last to corrode (Fig. 3a and b).

3.2. Unalloyed copper inclusions

Both Italian and Chinese artefacts showed the presence of UCI. In most cases UCI were located in the core of the artefacts, far from the outer corrosion products layer, and were often connected to interdendritic corrosion zones (Figs. 5 and 6). The black interdendritic corrosion areas adjacent to UCI appeared scarlet-red under

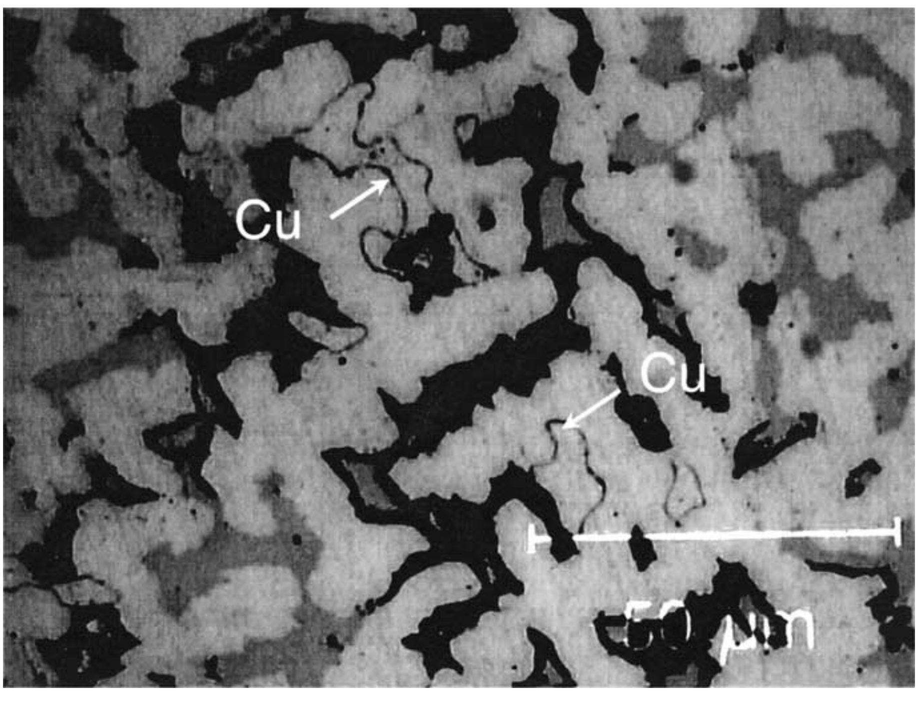

Figure 5 Unalloyed copper ("Cu") replacing the corroded eutectoid in the brooch R2, unetched.

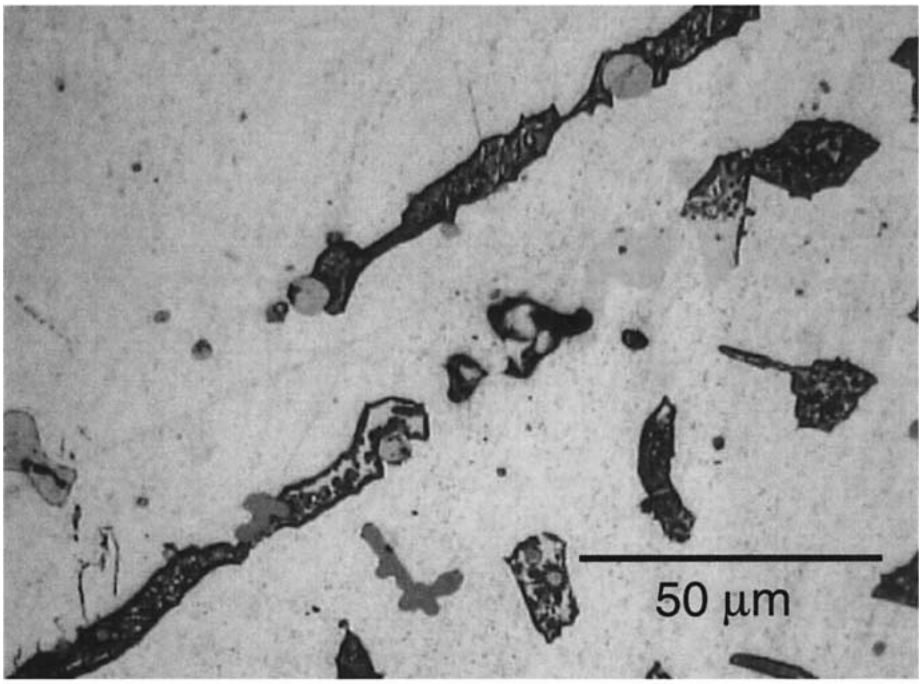

(a)

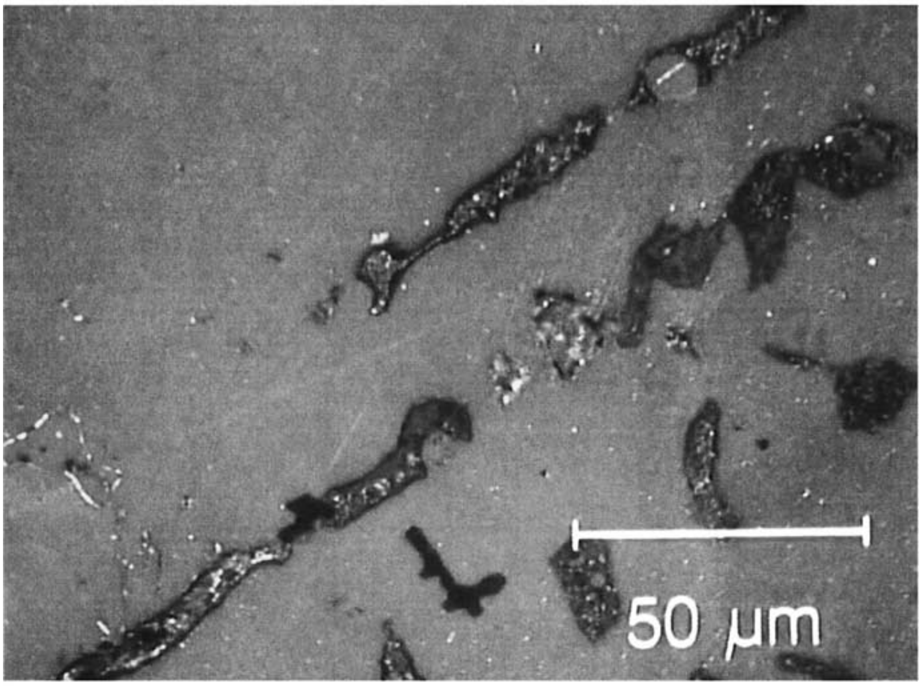

(b)

Figure 6 Corroded areas adjacent to copper globules in the blade of the knife R8 (unetched): bright-field (a) and reflected polarised light image (b).

polarised light (Fig. 6); their tin content was variable and generally low, decreasing to extremely low amounts in the most corroded regions (Fig. 7).

The size of the UCI ranges from a few microns (Figs 6–11) to hundreds of microns (Figs 3a and 12). The shape of UCI varied from the circular shape of the smaller ones (Figs 6, 10 and 11) to the irregular shape of the ones occupying the interdendritic areas around the α-phase (Figs 3a, 5 and 12).

UCI were often adjacent to copper sulphides (Fig. 3b); a crown of copper sulphides surrounded some UCI (Figs 10 and 11). In Chinese vessels, UCI were also close to lead globules (Fig. 9).

UCI sometimes displayed a twinned grain structure (Figs 3a and 12); small UCI can be found in zones where twinned grains are present in the α-phase (Fig. 8a). However, most UCI are located in the dendritic region.

In the case of knife R8, an interdendritic crack, which penetrated deeply into the structure, was filled by unalloyed copper (Fig. 13). UCI were present in interdendritic areas around the crack.

4. Discussion

Both the objects described in the literature and those studied in this work were characterised by (i) having

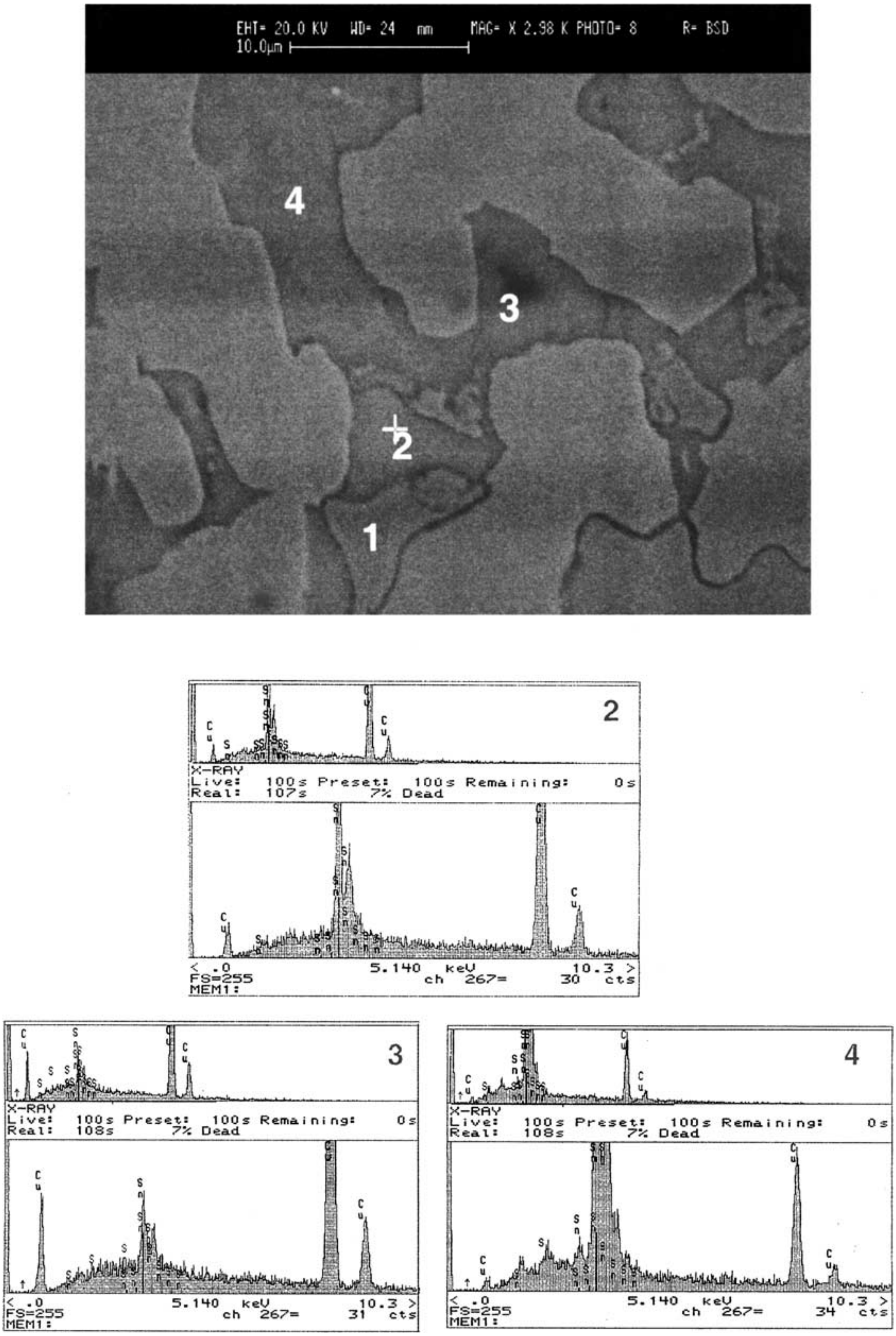

Figure 7 Variation of the Sn content (EDS spectra 2–4) around UCI (labelled 1in the SE image, upper left) in the eutectoidic area (brooch R2).

an $\alpha/\alpha + \delta$ structure with dendritic zones; (ii) coming from a burial environment where preferential corrosion left most of the α-phase unattacked.

Different types of UCI were observed in the examined samples. Differences in UCI morphology and distribution can be ascribed to different formation mechanisms. Therefore the different types of UCI can be classified as follows:

- type-A UCI: irregularly shaped UCI, that pseudomorphically replace other phases;
- type-B UCI: globular UCI, that are surrounded by a layer of copper sulphide;
- type-C UCI: large, irregularly shaped UCI, that display a twinned microstructure. Examples of type-A, -B and -C UCI can be seen in Figs 5, 10 and 3a respectively.

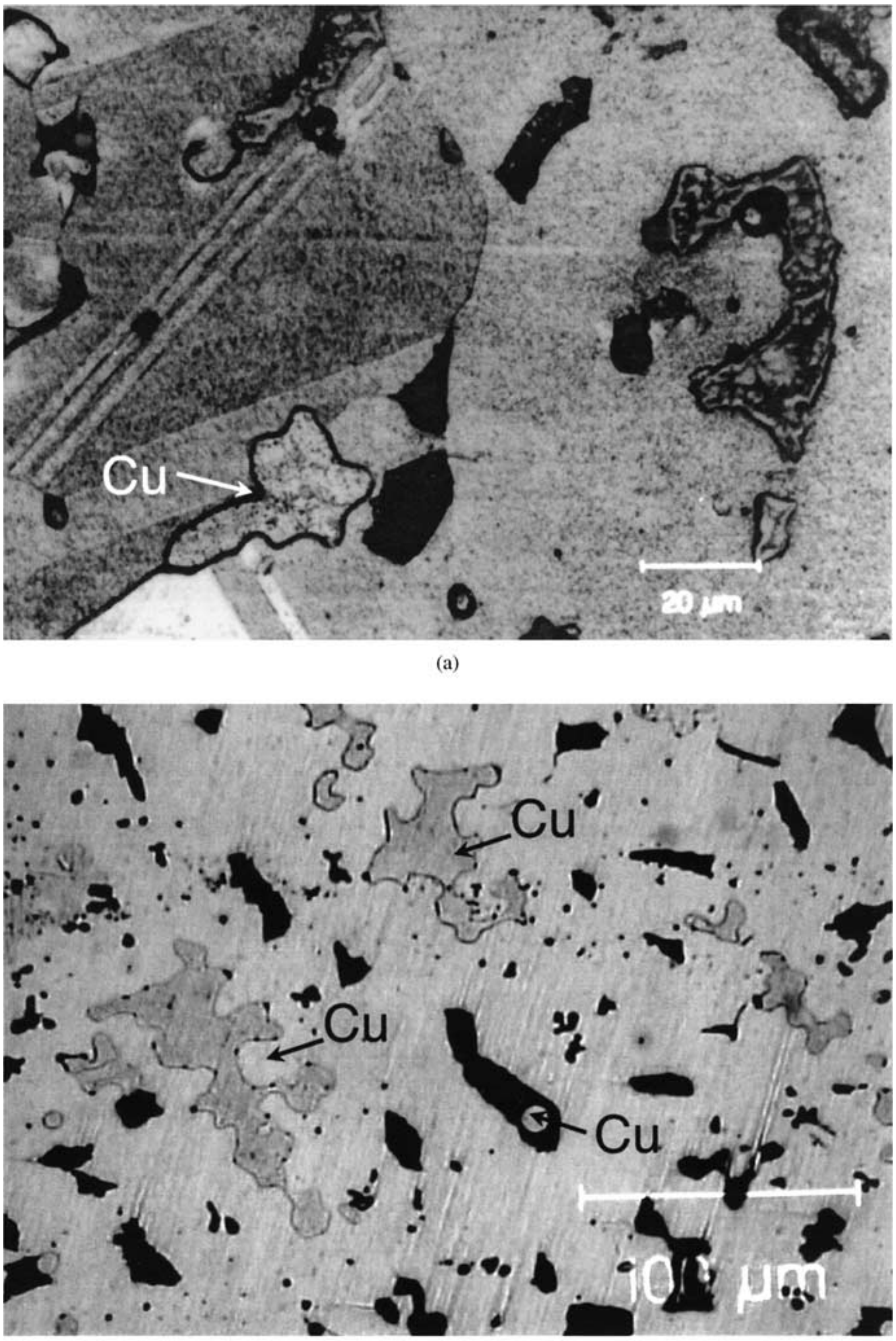

Figure 8 Unalloyed copper patches ("Cu") in the blade of the sword R1 (a, etched with $FeCl_3$/HCl/ethanol) and the knife R8 (b, unetched).

4.1. Type-A UCI
Extensive interdendritic corrosion of the $\alpha + \delta$ eutectoid was observed in the bronze artefacts that contain type-A UCI (Fig. 5). This is not surprising, since tin-rich phases are known to oxidise preferentially in tin bronzes exposed to a low-oxygen environment. In the observed Italian objects, the interdendritic spaces in the inner zone of the cross section are filled by UCI more extensively than the ones in the peripherical zone, where UCI are partly surrounded by dark corrosion zones (Figs 6 and 8b). The dark zones produced by the corrosion of the eutectoid contain copper and, to a lesser extent, tin. The tin content in the corrosion zones (black areas) is lower than in the uncorroded eutectoid (Fig. 7). According to the corrosion-redeposition mechanism proposed by [4, 8], these UCI might be the result of the first stages of the transformation of cuprite to redeposited copper in the interdendritic corrosion zones. According to E-pH diagrams for copper [16], the reduction of cuprite to copper begins when the oxidising potential and /or pH drops. The oxidising potential decreases from the surface towards the core of the objects because of both the consumption of oxygen in the oxidation processes on the surface and the presence of corrosion layers. This might account for the prevalence of UCI in the core regions of the objects, where it is more difficult for oxygen to penetrate.

Wang and Merkel suggest in a recent paper [11] that the central question concerning metallic copper in bronzes is whether it is redeposited copper or the result

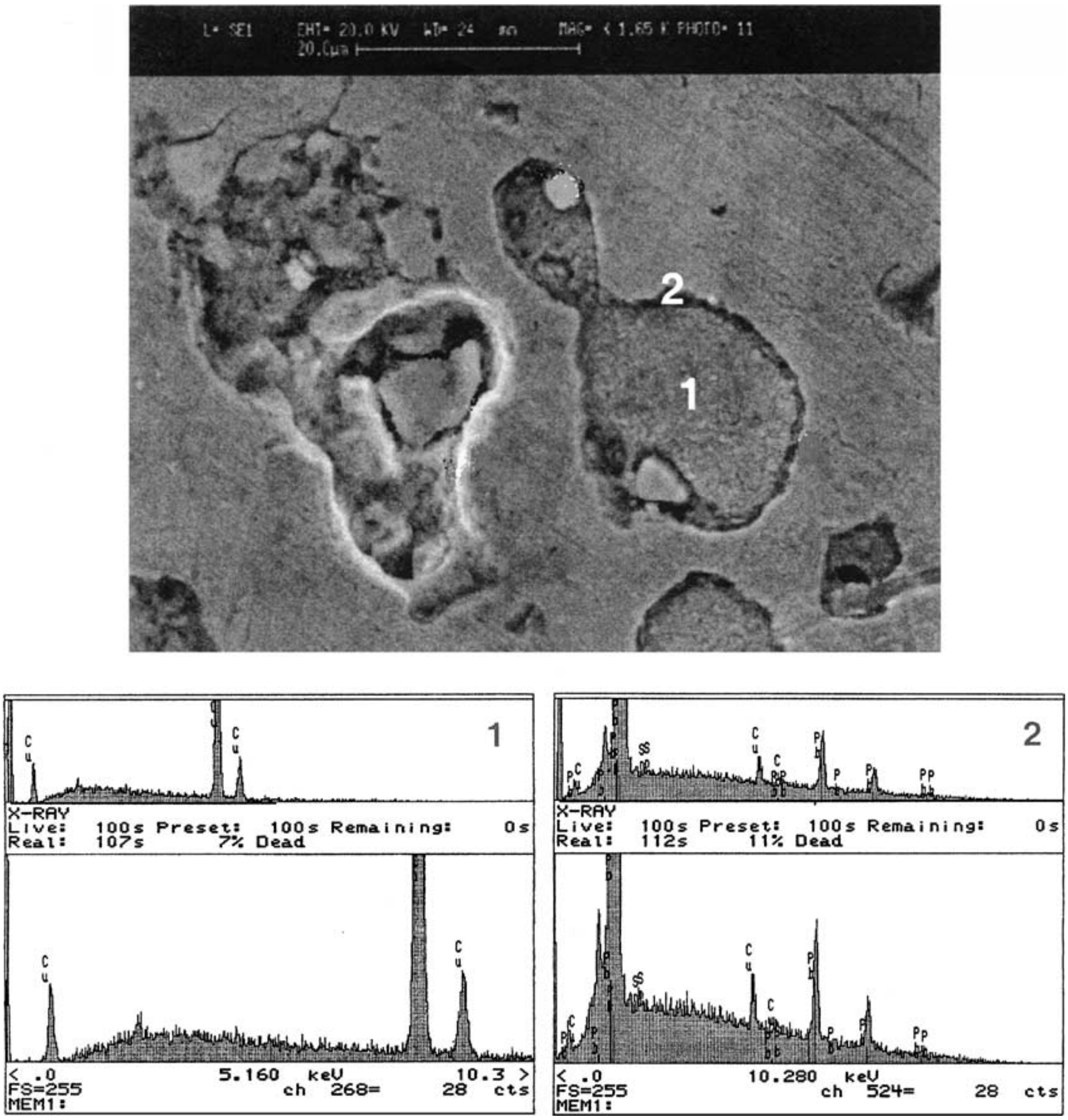

Figure 9 Unalloyed copper globule (1) with remnants of a lead globule (2) in the *Hu* pot 1A.

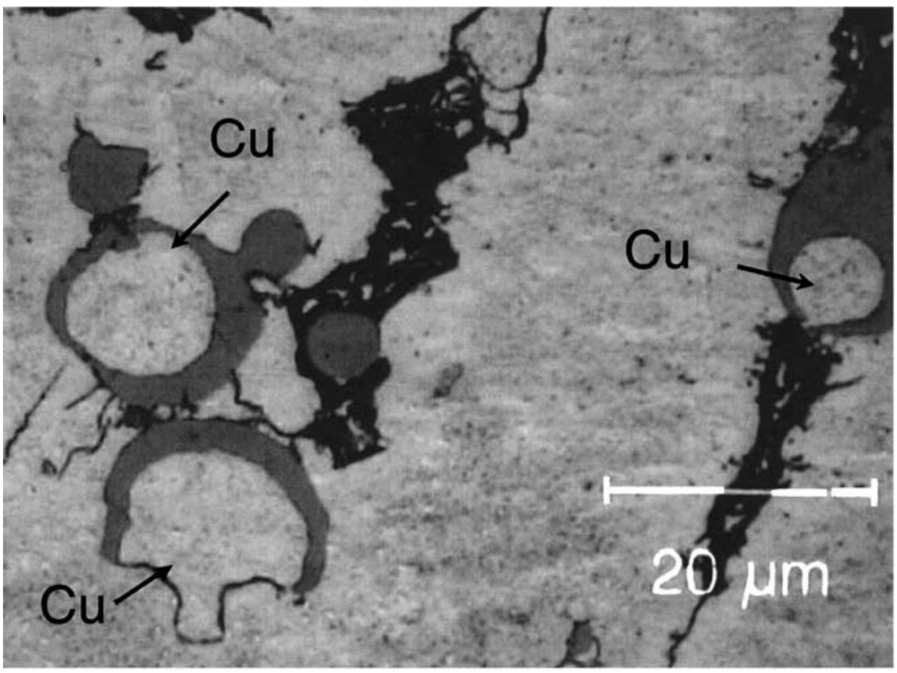

(a)

Figure 10 Copper spheroids ("Cu") surrounded by copper sulphides in the *Zun* vessel 1B: unetched (a) and etched with $FeCl_3$/HCl/ethanol. (*Continued.*)

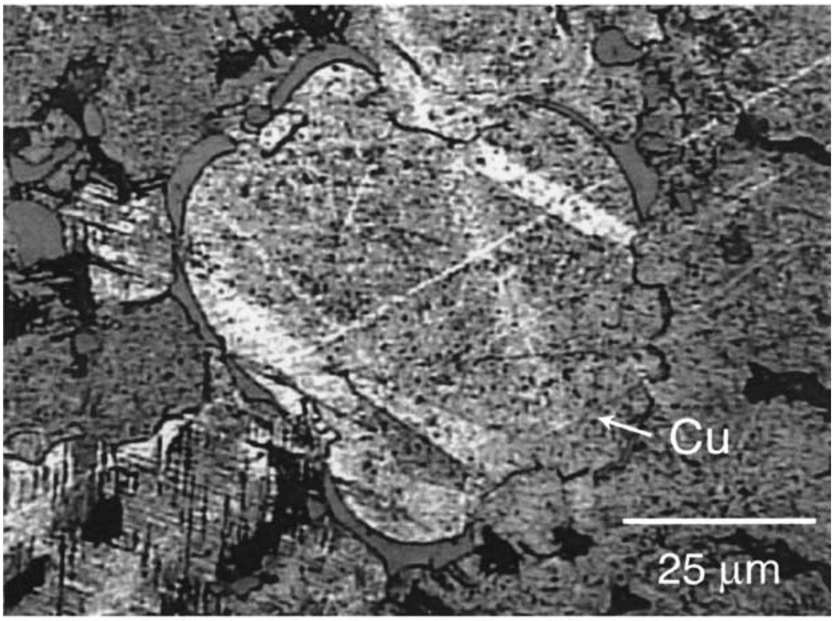

(b)

Figure 10 (*Continued*).

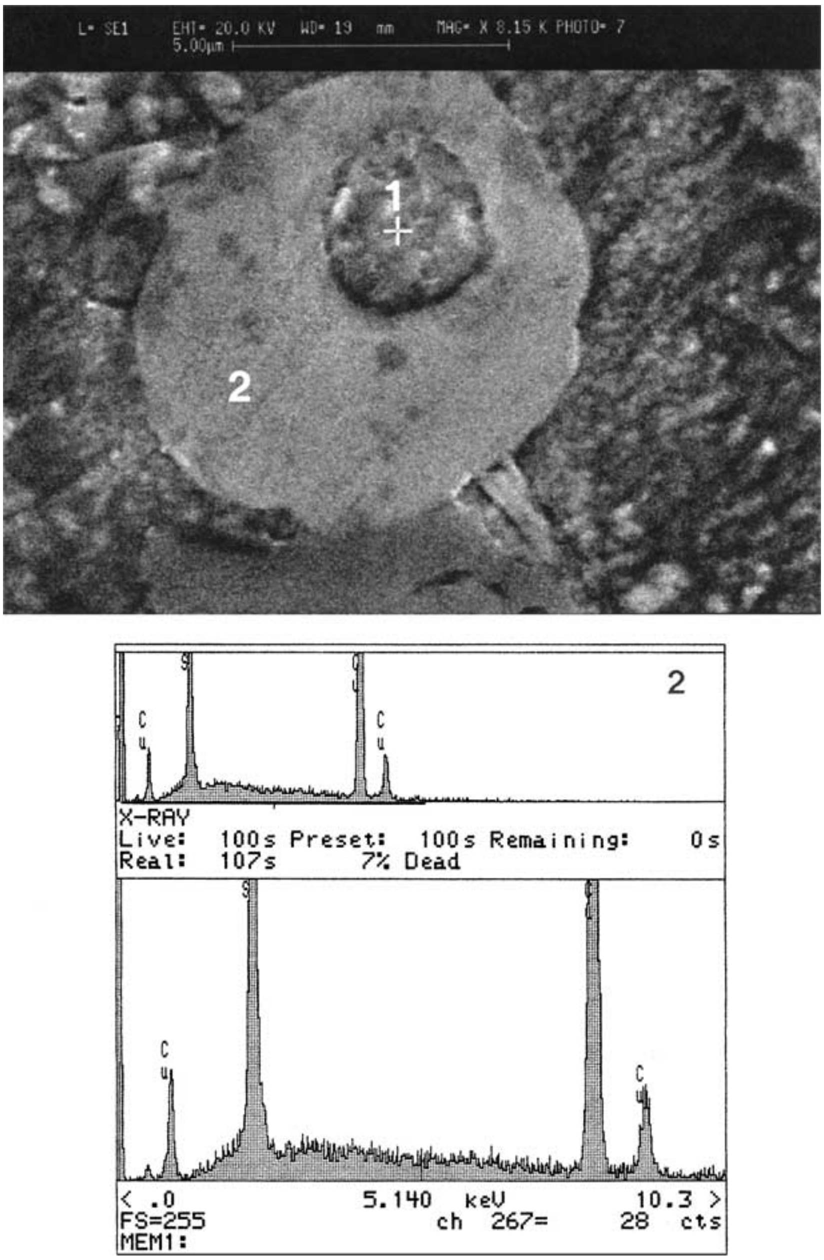

Figure 11 Copper spheroids (1) surrounded by copper sulphides (2) in the *Zun* vessel 1B.

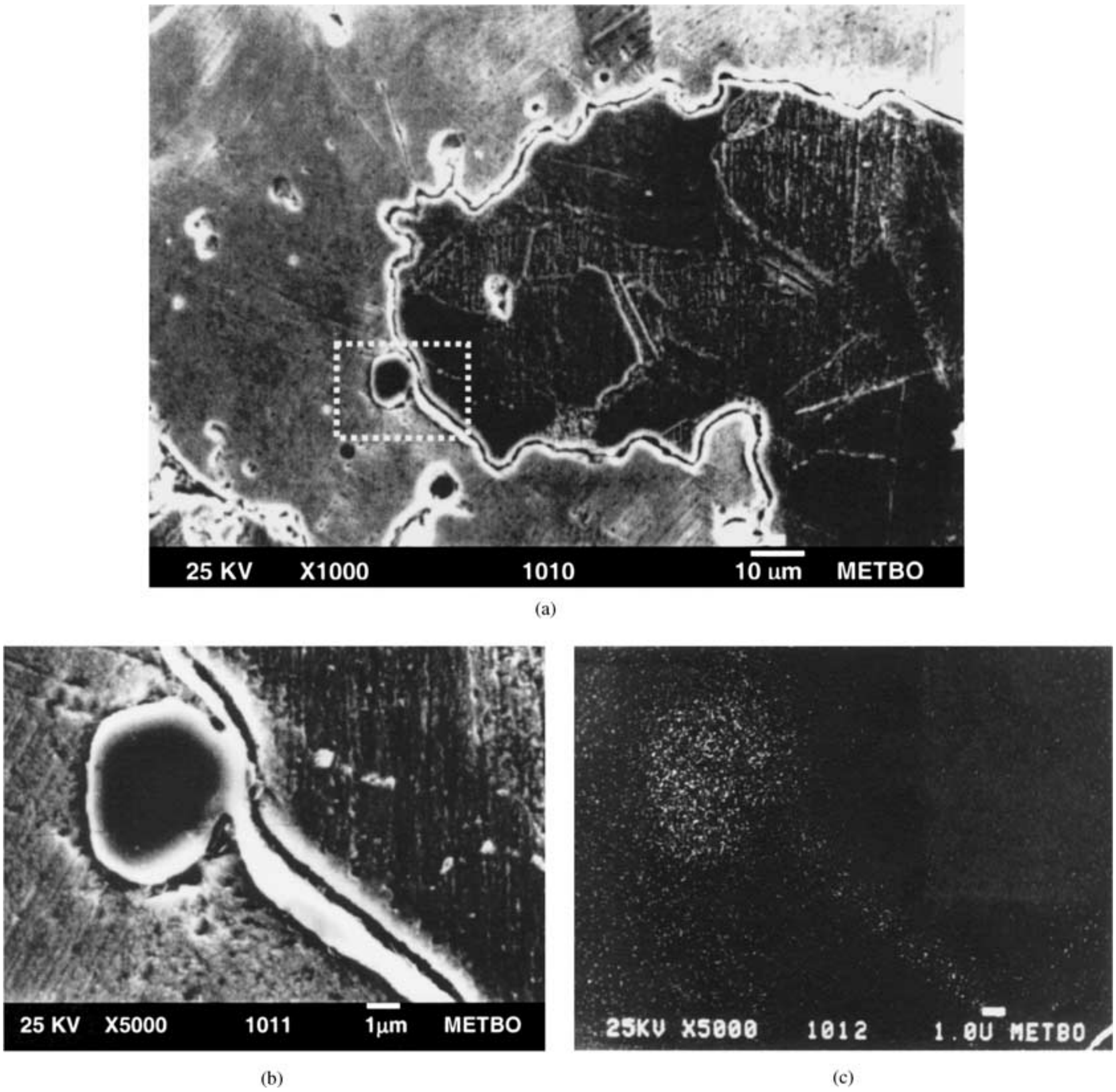

Figure 12 Blade of the sword R1: a large copper globule with twinned grains: (a) SE image, (b) detail of the grain boundary in the dotted area of image (a) and (c) sulphur (S K_α) X-Ray map of the image (b).

of destannification, where destannification is defined as selective removal of tin leaving residual copper. They suggest that "metallic copper producing pseudomorphs of the original structure, e.g., eutectoid of $(\alpha + \delta)$, should be considered destannification (...) while copper formed in pre-existing cracks or voids and within any other corrosion products (...) should be considered redeposited copper". The distinction between destannification and redeposition is based on the assumption that destannification does not involve dissolution of copper, whereas it was demonstrated that in the case of dezincification the dissolution of both copper and zinc was followed by the redeposition of copper [17]. To our opinion, type-A UCI are likely to be the result of the copper corrosion-redeposition mechanism described in the introduction. The most common type of A-UCI are the interdendritic patches of copper that replace the $\alpha + \delta$ eutectoid, but redeposited copper might replace (i) the corroded eutectoid or (ii) corroded lead globules (in leaded bronzes) or (iii) copper corrosion products, for instance cuprite (e.g., in trough-thickness cracks or beneath corrosion product layers, see Table I). Unfortunately, it was impossible to draw representative samples of the corrosion products on the objects, therefore we have no information on the *patina*, and the lack of scientific data concerning the burial environment (i.e., pH, redox potential, presence of cations/anions or bacteria) doesn't allow a more comprehensive interpretation of the deterioration mechanism.

4.2. Type-B UCI

The spherical morphology of type-B UCI (Figs 10a and 11) suggests that they might originate from a liquid phase. Furthermore, the presence of a copper sulphide "crown" around type-B UCI suggests that they might have formed during roasting of the copper ore. If we assume to use copper sulphides, e.g., chalcocite (Cu_2S), as a copper source, interactions between cuprous oxide formed by oxidation of Cu_2S and the remainder of Cu_2S can be described by the following reaction [18]:

$$Cu_2S + 2Cu_2O \rightarrow 6\,Cu + SO_2 \qquad (1)$$

According to the Cu-S phase diagram [19], if the temperature is higher than 1105°C two immiscible liquids exists when the sulphur content is lower than 20% wt. As these liquids have different densities the

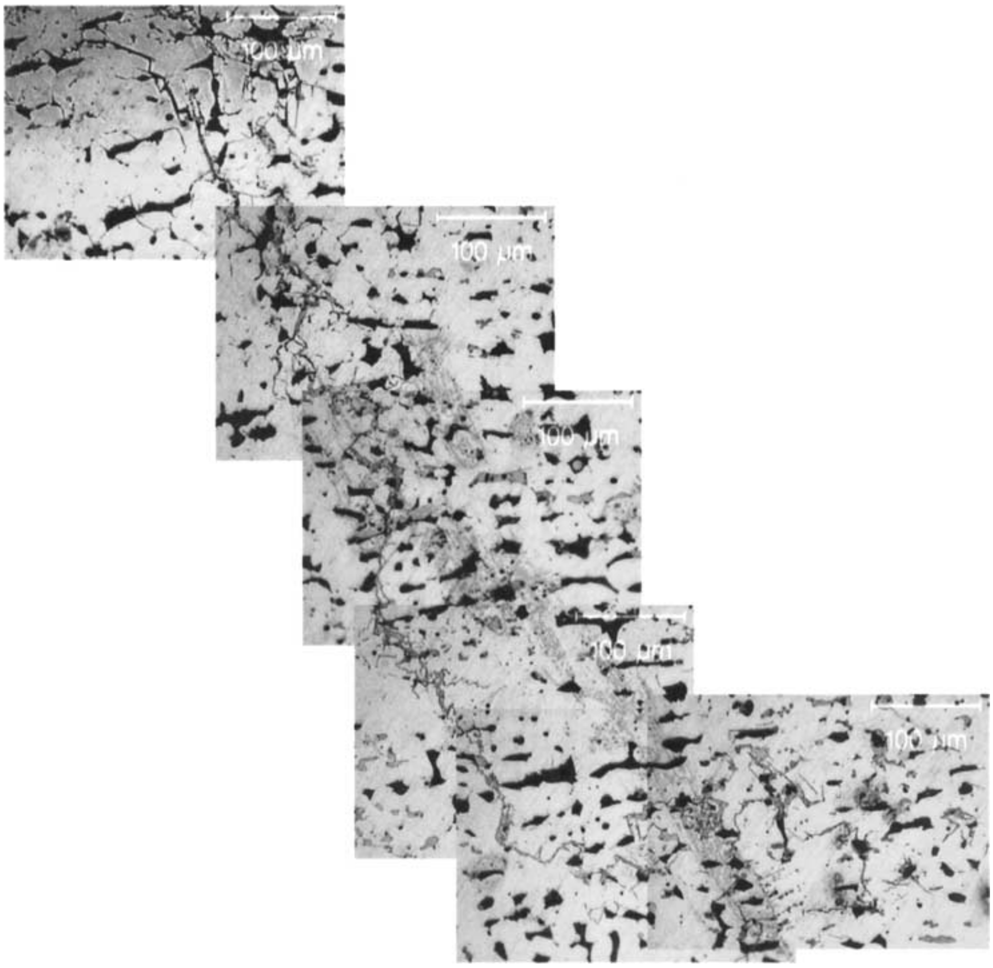

Figure 13 Through-thickness crack in the cross section of the blade of knife R8, unetched; the external surface of the blade is close to the upper left corner of the sequence of OM images. The crack is filled by unalloyed copper (dark grey), mainly in the inner region of the sample. Patches of unalloyed copper (dark grey) are present in interdendritic spaces around the crack (third picture from the top, on the right).

melt separates into a top layer with a composition that corresponds to Cu_2S, and a bottom layer of Cu with about 2% wt. of dissolved sulphur (copper-rich Cu-S solution). On cooling below 1105°C, the solid phase Cu_2S and the copper-rich Cu-S solution are present. In these conditions, slagging of solid Cu_2S should take place, in order to obtain high-purity copper. Spherical particles of Cu_2S containing a copper-rich core might form during cooling; these spheroids are heavier that Cu_2S particles and therefore are less likely to slag properly. Copper-rich globules coated with a copper sulphide layer might consequently remain in the alloy and form type-B UCI.

4.3. Type-C UCI

Type-C UCI are very large (more than 50 μm dia.) and are not located close to other phases that might be replaced by redeposited copper. Also the non-spherical morphology and the absence of a thick sulphide layer around type-C UCI (Fig. 3a), suggest that these inclusions are due to incomplete mixing of copper and tin during casting of the alloy. Twinned copper grains (Fig. 12), that have been observed in the bronze matrix also by other authors [5, 9], are likely to be generated in type-C UCI during cooling, in agreement with the hypothesis that type-C UCI existed in the microstructure of the artefacts before the beginning of corrosion phenomena, as the result of incomplete mixing during casting of the alloy.

5. Conclusions

UCI (Unalloyed Copper Inclusions) have been observed in many bronze artefacts with very different features and purposes. UCI observed in the investigated archaeological bronzes as well as those described in the literature have been compared and discussed. UCI were classified on the basis of their morphology and distribution: three main types of UCI were identified and a formation mechanism has been proposed for each type of UCI.

The formation of type-A UCI is closely related to long-term corrosion processes, whereas type-B and -C UCI were probably already present in the artefacts before corrosion took place.

Acknowledgments

The Authors wish to thank Prof. G. Brunoro, University of Ferrara as well as Prof. O. Ruggeri and Prof. G. P. Cammarota of the University of Bologna for helpful discussions. Dott. A. Cardarelli, Museo Archeologico Etnologico, Modena, Italy, is gratefully acknowledged for kindly providing the artefacts from the "Terramare" culture. Dr. Zhang Xiaomei of the University of Beijing, China, is gratefully acknowledged for contributing to the study of Chinese vessels. The research has been carried out with the financial support of CNR (National Research Council of Italy) under Special Project "Cultural Heritage".

References

1. I. DAVY, *Philosophical Transactions of the Royal Society of London* **16**(2) (1826) 65.
2. R. J. GETTENS, in "The Freer Chinese Bronzes," Smithsonian Institution Freer Gallery of Art Oriental Studies No. 7, Vol. II, Technical Studies, Smithsonian Publication 4706 (Smithsonian Institute, Washington, USA, 1969) p. 121, 177.
3. R. GOLDSTRAW, *Conservation News* **31** (1986) 13.
4. D. A. SCOTT, in "Metallography and Microstructure of Ancient and Historic Metals" (The J. P. Getty Trust, Los Angeles, USA, 1991) p. 92, 94, 111.
5. M. LEONI, M. DIANA, G. GUIDI and F. PERDOMINICI, *La Metallurgia Italiana* **83**(11) (1991) 1033.
6. N. A. NIELSEN, in "Corrosion and Metal Artifacts—A Dialogue between Conservators and Archaeologists and Corrosion Scientists," edited by B. F. Brown, H. C. Burnett, W. T. Chase, M. Goodway, J. Kruger and M. Pourbaix (NACE, Houston, Texas, USA, 1991) p. 17.
7. WANG CHANGSUI, WU YOUSHI, FAN CHONGZHENG, WANG SHENGJUN and HUA JUEMING, in Proceedings of the EEC China Workshop on Preservation of Cultural Heritages, Xian, Shaanxi, People's Republic of China, Sept. 25–30, 1991 (Teti, Napoli, 1992) p. 502.
8. W. T. CHASE, in "Ancient and Historic Metals," edited by D. A. Scott, J. Podany and B. B. Considine (The Getty Conservation Institute, Los Angeles, USA, 1994) p. 85.
9. JIA YING, SU RONGYU, HUA JUEMING, LINGMU REN, HUANG YUNLAN and XIAO MENGLONG, *Sciences of Conservation & Archaeology* **11**(2) (1999) 31.
10. K. TRENTELMAN, L. STODULSKI, R. LINTS and CHONGMIN KIM, *Studies in Conservation* **44** (1999) 170.
11. WANG and MERKEL, *Studies in Conservation* **46** (2001) 242.
12. H. ZITTER and K. PAULUZZI, *J. Mater. Sci.: Mater. Med.* **4** (1993) 159.
13. ZHANG XIAOMEI, YUAN SIXUN, LIU YU and ZHOU BAOZHONG, *Sciences of Conservation and Archaeology* **11**(2) (1999) 7.
14. M. R. COWELL, P. T. CRADDOCK and M. J. HUGHES, *Archaeometry* **18**(1) (1976) 19.
15. G. L. GARAGNANI, V. IMBENI and C. MARTINI, in "Le Terramare—La più antica civiltà padana" (Electa, Milano, 1997) p. 554.
16. M. POURBAIX, in "Corrosion and Metal Artifacts—A Dialogue between Conservators and Archaeologists and Corrosion Scientists," edited by B. F. Brown, H. C. Burnett, W. T. Chase, M. Goodway, J. Kruger and M. Pourbaix (NACE, Houston, Texas, USA, 1991) p. 1.
17. L. L. SHREIR, in: "Corrosion—Metal Environment Reaction, Vol. 1" (Newnes Butterworths, London) p. I: 167.
18. A. A. TSEIDLER, in "Metallurgy of Copper and Nickel" (Israel Program for Scientific Translations Ltd., Jerusalem, Israel, 1964) p. 107.
19. "ASM Handbook, Vol. III: Alloy Phase Diagrams" (ASM International, Metals Park, OH, USA, 1992) p. 2 · 177.

Received 6 March
and accepted 5 June 2002